(NASA-CR-143947) JUNCTION ROUGHNESS LEVEL INTEGRAL MATRIX ESCALIBER Final Report (Aerotherm Acurex Corp., Mountain View) 43 p HC $3.75 CSCL 20D

N75-32019

Unclas
G3/32 35841

AEROTHERM
ACUREX Corporation

Aerotherm Project 6383

July 1975

JANNAF BOUNDARY LAYER INTEGRAL MATRIX PROCEDURE

R. Michael Evans

Aerotherm Division/Acurex Corporation
Mountain View, California 94042

AEROTHERM FINAL REPORT 75-152

Prepared for

National Aeronautics and Space Administration
George C. Marshall Space Flight Center
Marshall Space Flight Center, Alabama 35812

Contract NAS8-30930

Technical Monitor: Klaus Gross

ABSTRACT

A summary of modifications to the JANNAF version of Aerotherm's Boundary Layer Integral Matrix Procedure (BLIMP-J) is presented. The BLIMP-J program is the standard prediction method for boundary layer effects in liquid rocket engine thrust chambers. One of these modifications, the addition of the turbulent models of Cebeci and Smith and of Bushnell and Beckwith, is discussed in detail. Comparisons of the predictions of these models and the model of Kendall between the models and with data are also presented. The Cebeci-Smith and Bushnell-Beckwith models are in close agreement for all cases studied. For the case of large values of T_e/T_w (≈ 5) the Kendall model does not agree with the other two. It is recommended that the Kendall model remain as the turbulent model for use in the standard prediction procedure until sufficient comparisons with appropriate high temperature ratio data are made. Recommendations for future work are alos presented.

TABLE OF CONTENTS

LIST OF ILLUSTRATIONS

LIST OF SYMBOLS

A	constant used in Cebeci model = 26
A^+	defined by Equation (13) for Cebeci model; = 26 for Bushnell model
B	constant in Cebeci model = 34
B^+	defined by Equation (16)
c	constant used in expression for wake eddy viscosity
k,K	constant in the mixing length expression
ℓ	mixing length
M	Mach number
MR	mixture ratio
P	pressure
Pr	Prandtl number
R	radius
Re_Θ	Reynolds number based on momentum thickness
Sc	Schmidt number
T	temperature
u	velocity in streamwise direction
u_τ	friction velocity = $\sqrt{\tau_w/\rho}$
v	velocity normal to the wall
x	axial coordinate or local streamwise coordinate
y	coordinate normal to the wall
y_a^+	constant used in Kendall model = 11.823
y^+	= $y\sqrt{\tau_w/\rho}/\nu$

δ^*	velocity defect = $\int_0^\infty (1 - u/u_e)\, dy$
ε_D	eddy diffusivity
ε_h	eddy conductivity
ε_m	eddy viscosity
ε_r	reference value of eddy viscosity
θ	momentum thickness
μ	molecular viscosity
ν	molecular kinematic viscosity
ρ	density
τ	shear stress

Subscripts

e	edge value
o	stagnation value
T	throat value
t	turbulent value
w	wall value

Superscript

$'$	turbulent fluctuation

SECTION 1

INTRODUCTION

Accurate predictions of the thrust loss due to boundary layer effects and of the wall heat flux are very important to the design and performance evaluation of rocket nozzles. The JANNAF version of Aerotherm's Boundary Layer Integral Matrix Procedure (BLIMP-J) is the reference method in the recommended rigorous analytical procedure for rocket engine performance prediction and evaluation (Reference 1). The JANNAF version of the BLIMP program has been specially modified for easy interface with other programs of the JANNAF recommended procedure. The BLIMP-J program is a fast and accurate procedure for solving the set of boundary layer equation (momentum, energy, and species) for laminar or turbulent, chemically reacting flows with a wide variety of boundary conditions. This computer program has been fully documented and its use described in Reference 2.

In this report the most recent improvements to the BLIMP-J program are described and the results of comparison of the turbulent models of Kendall (References 3 and 4), Cebeci and Smith (References 5 and 6) and Bushnell and Beckwith (References 7 and 8) are presented. Section 2 contains a summary of the recent modifications and additions to the program. The turbulent models and the results of the comparisons are given in Section 3. Conclusions and recommendations for future work are presented in Sections 4 and 5.

SECTION 2

CODE MODIFICATIONS

This section contains a brief discussion of the additions and modifications made to the BLIMP-J program since the conclusion of a previous updating (Reference 9). Details of these modifications and the entire BLIMP-J program can be found in Reference 2.

2.1 HOMOGENEOUS GAS OPTION

It is frequently desired to make fast preliminary boundary layer calculations or to make calculations for air flow models where no chemical reactions take place. To facilitate these calculations a homogeneous, or nonreacting, gas option has been added to the program. In this option the gas species composition is specified by the user and is not allowed to change. Additionally, the gas viscosity and Prandtl number as functions of temperature are specified by the user. In this way the species equations are eliminated from the set of boundary layer equations and the complex equilibrium chemistry and transport property routines are replaced by very simple calculational procedures. This can greatly reduce the execution time and, in the case of low temperature air, provide greater accuracy through improved transport property values (μ, Pr) at low temperatures.

2.2 BINARY DIFFUSION OPTION

Another simplification useful for reducing the execution time for problems with more than two elements in the chemical system is the binary diffusion option (see Section 2.4 and 6.4 of Reference 2). The use of this option reduces the number of species equations to one from a maximum possible of seven. This can result in a 40 to 75 percent savings in total execution time, depending on the number of elements in the gas. (A typical problem might require 20 to 30 minutes (Univac 1108) without the binary diffusion option.)

The effect of this option on the solution depends on the degree to which unequal molecular diffusion is important to the accuracy of the solution. For turbulent flow problems with no blowing the effects may be, and usually are, small.

2.3 LOW TEMPERATURE RANGE

In certain cases where very large expansion ratios are encountered, it is sometimes the case that the gas temperature may vary over a wide range. A third range for thermodynamic curve fit constants has been added to allow for more accurate thermodynamic properties determination. This range is only used when specifically requested by the user.

2.4 EXPANDED NAMELIST INPUT

The input for the BLIMP program has been modified to accept namelist input for most of the input. This option facilitates minor changes to data decks as an aid to the user. Many input values have been preprogramed for standard default values when used with the namelist options. The complete formatted input has also been retained.

2.5 MISCELLANEOUS MODIFICATIONS

2.5.1 Plot Output

Optional output to a plot file of many key parameters has been added. The boundary layer edge values, integral parameters, and boundary layer profiles can be stored (either on the file or on tape) for use with a plot routine. No plot routine is supplied with the program. The exact format of the plot file is described in Section 7.5 of Reference 2.

2.5.2 Boundary Layer Flow Rate

The mass flux in the boundary layer has been added as output. This was done so that comparison could be made with the mass flux in the wall zone of the TDK (Reference 10) solution. It is desirable to have the edge of the boundary layer contained within the wall zone of the TDK solution.

2.5.3 Edge Conditions

The edge conditions for the boundary layer solution were previously calculated from a given stagnation condition and edge pressure distribution for an isentropic expansion. This has now been expanded to allow for a nonisentropic expansion whereby the edge thermodynamic state can be calculated from either pressure and velocity or pressure and entropy. In addition the edge pressure gradient and edge velocity gradient can be input directly if desired.

2.5.4 Convergence Criteria

The convergence criteria for the boundary layer equations was reformulated to be self-adjusting for boundary layers with large streamwise pressure gradients or rapidly changing

boundary layer shape and thickness. These criteria compare the errors in the momentum, energy, and species equations (see Section 3 of Reference 2) to a relatively small number which is adjusted according to certain parameters in the equations. The present methods have proved to be very reliable for all types of problems considered.

SECTION 3

TURBULENT MODELS STUDY

The prediction of wall heat flux, momentum thickness, and displacement thickness for turbulent boundary layers is very dependent upon the turbulent model employed in the prediction tool. The original turbulent model in the BLIMP code was developed by R. M. Kendall, has been described in previous BLIMP documentation (References 4 and 11), and has extensive use for both external and internal flow predictions. There are many other models in use for turbulent predictions. Two of these, by Cebeci and Smith (References 5 and 6) and Bushnell and Beckwith (References 7 and 8), were selected to be added to the BLIMP code. This would make possible a comparison of three of the leading turbulent models of the mixing length type in the same computational routine for general equilibrium chemistry and a broad range of possible boundary conditions.

In Section 3.1, the basic formulation of each of the three turbulent models is given. In Section 3.2, a comparison of the three models is presented. The execution time for the three models is compared in Section 3.3.

3.1 THE TURBULENT MODELS

The general features of the turbulent models are described in Section 3.1.1 and each model is described in detail in the subsequent sections.

3.1.1 General Features

Bossinesq's eddy viscosity concept is adapted to write the Reynolds stresses as

$$\overline{-(\rho v)'u'} = \rho\varepsilon_m \frac{\partial u}{\partial y} \tag{1}$$

and a similar relation is used to define eddy conductivity, ε_h

$$\overline{-(\rho v)'T'} = \rho\varepsilon_h \frac{\partial T}{\partial y} \tag{2}$$

All the three models under present discussion employ the Prandtl mixing length hypothesis in which it is assumed that

$$\varepsilon_m = \ell v_t \tag{3}$$

where ℓ is the mixing length and v_t is the turbulent velocity. The differences between the three models comes about through the formulation of ℓ and v_t. Kendall and Cebeci treat the boundary layer as a composite layer consisting of inner and outer regions. In the inner region the turbulent velocity is written as

$$v_t = \ell \left| \frac{du}{dy} \right| \tag{4}$$

and the mixing length is assumed to be proportional to the distance from the wall. In the outer or wake region, the boundary layer is assumed to behave similarly to free turbulent shear flow with $v_t = u_e$, the free stream velocity, and $\ell = c\delta^*$ where c is a constant and δ^* is a boundary layer characteristic thickness taken as the velocity defect thickness. Thus,

$$\varepsilon_m = c u_e \delta^* \tag{5}$$

where

$$\delta^* = \int_0^\infty \left(1 - \frac{u}{u_e}\right) dy \tag{6}$$

Bushnell and Beckwith, however, treat the boundary layer as a single layer and apply Equation (4) throughout by introducing the intermittency concept in the definition of ℓ. The most fundamental differences in the models arise from the manner is which the mixing length expression is obtained. The Cebeci and Bushnell expressions originate from Prandtl's proposal that in the region of the development of turbulence.

$$\frac{d\ell}{dy} = k \tag{7}$$

which has solution

$$\ell = ky \tag{8}$$

From this solution many significant modifications have followed to account for the effect of variable properties, pressure gradient, Reynolds number, etc. It is significant that these modifications were made to the solution and not to the basic proposition as expressed by Equation (7). The Kendall model, on the other hand, originates from modifications to the basic proposition to account for the effects of variable properties (see Equation (10)). Thus, differences in the models might become more pronounced as the degree of property variation increased. This is exactly what is reflected in the comparisons presented in Section 3.2.

The turbulent transport of scalar quantities is treated the same way as momentum by introducing the concepts of eddy conductivity, ε_h, and eddy diffusivity, ε_D. Turbulent Prandtl and Schmidt numbers are defined as $Pr_t \equiv \varepsilon_m/\varepsilon_h$ and $Sc_t \equiv \varepsilon_m/\varepsilon_D$. Cebeci proposes an expression for Pr_t as a function of the distance from the wall but in the Kendall and Bushnell-Beckwith models Pr_t is assumed to be a constant. The turbulent Schmidt number is also taken to be constant in all the models.

3.1.2 Kendall Model

This model employs the two-layer concept of the turbulent boundary layer. The wall law is based on the following three concepts:

- $\lim_{y \to o} \ell = 0$
- $\lim_{y \to o} d\ell/dy = 0$
- Rate of increase of the mixing length with y is proportional to the difference between the value postulated by Prandtl (ky) and its actual value

$$\frac{d\ell}{dy} \sim (ky - \ell)$$

The proportionality factor in this relation is assumed to be dependent on the local shear stress and local kinematic viscosity

$$\frac{d\ell}{dy} = (ky - \ell) \frac{\sqrt{\tau/\rho}}{y_a^+ \nu} \tag{9}$$

where y_a^+ is a constant. The values of the constants k and y_a^+ recommended in this model are 0.44 and 11.823, respectively. These constants have been obtained by matching the predictions

with experimental data in incompressible turbulent boundary layers with and without blowing (Reference 11). (Physically k can be considered as a measure of the rate of growth of the mixing length with respect to distance from the wall and y_a^+ is a measure of the thickness of the laminar sublayer.) The validity of the model for flows with wall blowing and streamwise pressure gradient is argued on the basis of using the local flow properties, such as local shear, in the model.

For compressible flow, the wall law is modified as follows:

$$\frac{d\rho\ell}{dy} = \left[k \int_0^y \rho dy - \rho\ell\right] \frac{\sqrt{\tau/\rho}}{y_a^+ \nu} \tag{10}$$

where, instead of describing the length scale of a turbulent eddy, the mass of the eddy, $\rho\ell$, is related to the mass available between the wall and the point of interest. The constants k and y_a^+, however, are left at their incompressible values. The above integral-differential equation is solved numerically to obtain the local value of the mixing length ℓ.

In the wake region, it is assumed that the eddy viscosity is a constant and is given by Clauser's expression (Equation (5)) where c = 0.018. The wall and the wake regions are matched by the following procedure: the ε_m expression for the wall region is used until it exceeds the wake value at which point the wake value of ε_m is used for the remainder of the boundary layer thickness. This value is linearly damped in the outer-portions of the boundary layer so that a value of zero occurs at the boundary layer edge.

3.1.3 Cebeci-Smith Model

As was mentioned above, a two-layer model is also used by Cebeci and Smith. In the inner (wall region) the Van Driest (Reference 12) form of mixing length is now used:

$$\ell = k_m y \left[1 - \exp(-y^+/A^+)\right] \tag{11}$$

where

$$y^+ = y \sqrt{\tau_w/\rho}\,/\nu$$

Van Driest suggested constant values of 0.4 and 26 for the k_m and A^+, respectively. (These have essentially the same meaning as k and y_a^+ and were arrived at by comparison with incompressible air flow data.) In the Cebeci model, however, these constants are replaced by

functions accounting for pressure gradient, and blowing. Compressibility effects are also accounted for by using local values for μ and ρ.

For flows with pressure gradient and mass transfer, Cebeci replaced the wall shear in the damping parameter by τ_s which he obtained from the simplified form of the momentum equation in the sublayer (Reference 5):

$$\frac{d\tau_s}{dy} - \frac{V_w}{\nu_w}\tau_s = \frac{dp}{dx} \tag{12}$$

The solution of this equation at $y^+ = 11.8$ results in

$$A^+ = A\left\{-\frac{p^+}{V_w^+}\left[\exp(11.8\ V_w^+) - 1\right] + \exp(11.8\ V_w^+)\right\}^{-1/2*} \tag{13}$$

where

$$p^+ = -\frac{dp}{dx}\frac{\nu}{\rho_w u_\tau^3}\ ,\quad V_w^+ = \frac{V_w}{u_\tau}\ ,\quad u_\tau = \sqrt{\frac{\tau_w}{\rho}} \tag{14}$$

and $A = 26$.

Following Van Driest's approach to arrive at the mixing length formulation with a damping factor in the inner region, Cebeci derived the following expression for eddy conductivity:

$$\varepsilon_h = k_m k_h y^2\left[1 - \exp(-y^+/A^+)\right]\left[1 - \exp(-y^+\sqrt{Pr}/B^+)\right]\left|\frac{\partial u}{\partial y}\right| \tag{15}$$

where

$$B^+ = B\left\{\frac{-p^+}{V_w^+}\left[\exp(11.8\ V_w^+) - 1\right] + \exp(11.8\ V_w^+)\right\}^{-1/2} \tag{16}$$

and

$$k_h = 0.44\ ,\ B = 34$$

Cebeci (Reference 6) further agreed that the above values of k_m, k_h, A, and B are only satisfactory for large Reynolds number ($Re_\theta > 6000$), and he proposed functions of Re_θ for k_m, k_h, A, and B. There is some question as to the validity of the Re_θ dependence, particularly

*If $V_w^+ = 0$, $A^+ = A\{-11.8p^+ + 1\}^{-1/2}$

for compressible flows in nozzles. Furthermore, the model is completely adequate without this dependence;* for these reasons the constant values of k_m, k_h, A, and B are used.**

The turbulent Prandtl number ($Pr_t \equiv \varepsilon_m/\varepsilon_h$) is obtained from Equations (3), (4), (11), and (15);

$$Pr_t = \frac{k_m \left[1 - \exp(-y^+/A^+)\right]}{k_h \left[1 - \exp(-y^+\sqrt{Pr}\,/\,B^+)\right]} \tag{17}$$

Although Equations (11) and (15) are valid only in the boundary layer inner region, Cebeci shows that Equation (17) agrees satisfactorily with experimental data of References (13) through (15) throughout the boundary layer and, hence, it is so used.

In the wake region, Cebeci (Reference 6) uses the Clauser expression for eddy viscosity, Equation (5) with c = 0.0168. This expression is damped in the same way as in the Kendall model.

3.1.4 Bushnell-Beckwith Model

The Bushnell-Beckwith model is a single layer model which reduces to the Van Driest form of mixing length near the wall and is modified in the outer region by an intermittency factor γ (Reference 16). The mixing length expression is written as:

$$\frac{\ell}{\delta} = K \left[1 - \exp(-y^+/A^+)\right] f(y/\delta)\gamma^{1/2} \tag{18}$$

where

$$\gamma = \frac{1 - \mathrm{erf}\left[5(y/\delta - 0.78)\right]}{2} \tag{19}$$

and

$$f(y/\delta) = \tanh\left(\frac{k_m}{K}\frac{y}{\delta}\right) \tag{20}$$

and the constants are: $k_m = 0.4$, $K = 0.08$, $A^+ = 26$ (from incompressible flow comparisons). The boundary layer thickness δ appearing in Equations (18) through (20) is defined as the distance normal to the wall where the velocity ratio $(u/u_e) = 0.995$.

---

*Personal communication: Tuncer Cebeci, McDonnell-Douglas, Long Beach, California.

**In a later article (AIAA, Vol. 11, No. 1) Cebeci argues that k_m and A are constant.

The present model has been tested against experimental data by Bushnell and Beckwith (Reference 17). In their work, however, they use a different function than the one given by Equation (20). They assume that $f = y/\delta$ in the inner wall region, $y/\delta \leq 0.1$, and it is a function of the incompressible shape factor ($H \equiv \delta^*/\theta$) in the far wall region, $y/\delta \geq 0.3$. The values of f in the far wall region are obtained from a curve fit to experimental data of ℓ/δ versus H. In the interval $0.1 < y/\delta < 0.3$ a straight line is used to join the inner and far wall regions. Based on this model, Bushnell and Beckwith compared their predictions of flows with blowing and pressure gradient with experimental data of References 18 and 19. They report (Reference 17) that in the application of the model to flows with wall blowing, the effect of blowing could be accounted for only when the wall damping factor of Van Driest, A^+, was made an experimentally based function of the blowing rate. The present functional form of f, Equation (20), is based on the recommendation of Harris.*

As it is noted by Harris (Reference 8), based on the available data, there exists a lack of conclusiveness as to how the turbulent Prandtl number should be formulated in terms of local boundary layer parameters under different flow conditions. Therefore, a constant value of 0.9 is used for Pr_t in this model.

3.2 COMPARISONS OF THE TURBULENT MODELS

The BLIMP program has been previously verified for several sets of turbulent flow data (Reference 9). In these cases the turbulent model of Kendall was used. The predictions were in good agreement with the data for the air flow cases. Two of the cases reported in Reference 9 are used here for comparison of the turbulent models. In addition, several hypothetical cases are evaluated to examine potential differences in the models and one set of data for flow over a hemisphere cylinder with large values of T_w/T_w (≈ 5) is discussed

3.2.1 Back and Cuffel — Supersonic Nozzle with Heat Transfer

These experiments were carried out in a cooled, conical nozzle with a convergent and a divergent half angle of 10° at the Jet Propulsion Laboratory, California Institute of Technology (Reference 20). The air flow was tripped well upstream of the converging section so that the flow was fully turbulent throughout the nozzle. These flow conditions are relevant to conditions in rocket engines operating at thrust levels for which laminarization does not occur. Values of T_e/T_w vary between 0.7 and 2; therefore, density variations through the boundary layer should not cause significant differences between the models. Values of Re_θ were between 6000 and 15,000 and the Mach number at the exit was 3.55.

*Personal communication.

Static pressures, wall heat fluxes, and coolant-side wall temperatures were measured along the nozzle wall. Heat flux was determined by calorimetric measurements in circumferential coolant passages. Boundary layer surveys were made with a flattened pitot probe 0.000127 m (0.005 inch) in height and with thermocouple probes at five locations, two of which are shown in Figure 1.

Comparison between the models and, where possible, the data for the two stations shown in Figure 1 and for the wall heat flux throughout the nozzle are presented in the following paragraphs. All of the model predictions were done with identical conditions using the recommended values for the various input parameters. In addition, the Cebeci model was also used with variable turbulent Prandtl number.

Figure 2 shows the overall agreement of the models and the data as reflected by the wall heat flux. The only significant difference is for the variable turbulent Prandtl number case in the converging section of the nozzle. In Figure 3, the momentum thickness is shown for the various models. Again, the overall agreement is very good. Tables 1 and 2 and Figures 4 and 5 show the comparisons near the entrance to the converging section and near the exit to the diverging section. The agreement among the models and the data is again very good. In almost all instances the models are within 10 percent of each other, with some exceptions for the Cebeci model with variable turbulent Prandtl number. The heat flux to the wall is an indication of the near wall behavior and the momentum thickness reflects the general profile shape. Thus, the models appear to be in agreement in both respects. This is further evidenced by comparison of the eddy viscosity profile shown in Figure 6. Here it can be seen that throughout the portion of the boundary layer dominated by turbulence ($\varepsilon > \nu$) the models are in very close agreement. The differences in the laminar sublayer ($\nu > \varepsilon$) have little effect on the solution since the molecular viscosity dominates. The slight differences in the outer wake region also have little effect since the shear terms are small as a result of du/dy being very small.

3.2.2 Rocketdyne: O_2/H_2 Two-Dimensional Nozzle

This case* is representative of the type of data that can be expected from hot fired nozzles using O_2/H_2 fuel systems. The gas side wall temperature and the wall heat flux distributions were measured; however, no boundary layer measurements were made. Since heat flux is an important quantity and this case was for a representative liquid rocket fuel, it was

*The data for this case were supplied by Mr. George Osugi of Rocketdyne.

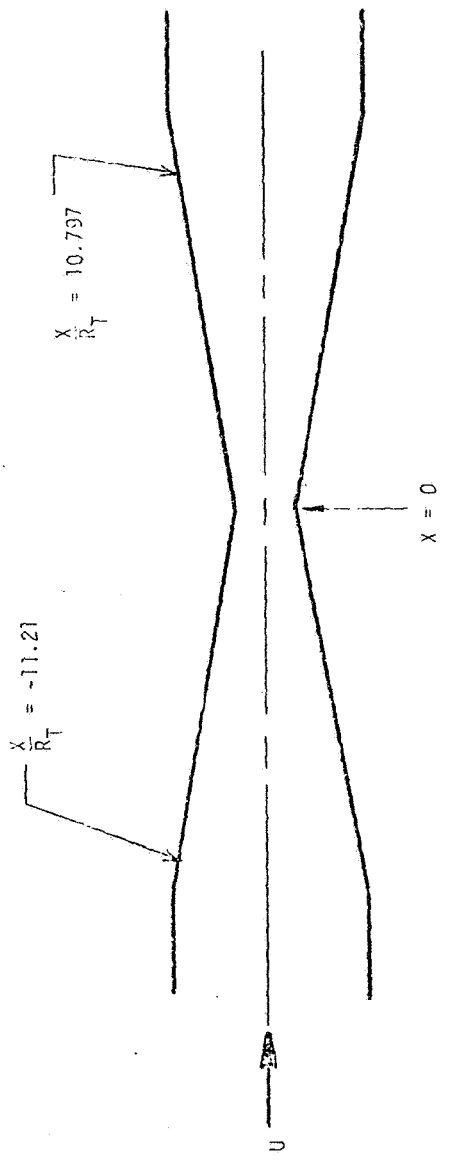

Figure 1. Schematic of Back and Cuffel nozzle showing boundary layer probe stations.

R_T = 0.0202 m (0.795 in.)

ε = 9.89

Nozzle length = (converging-diverging sections) = 0.51 m (20.07 in.)

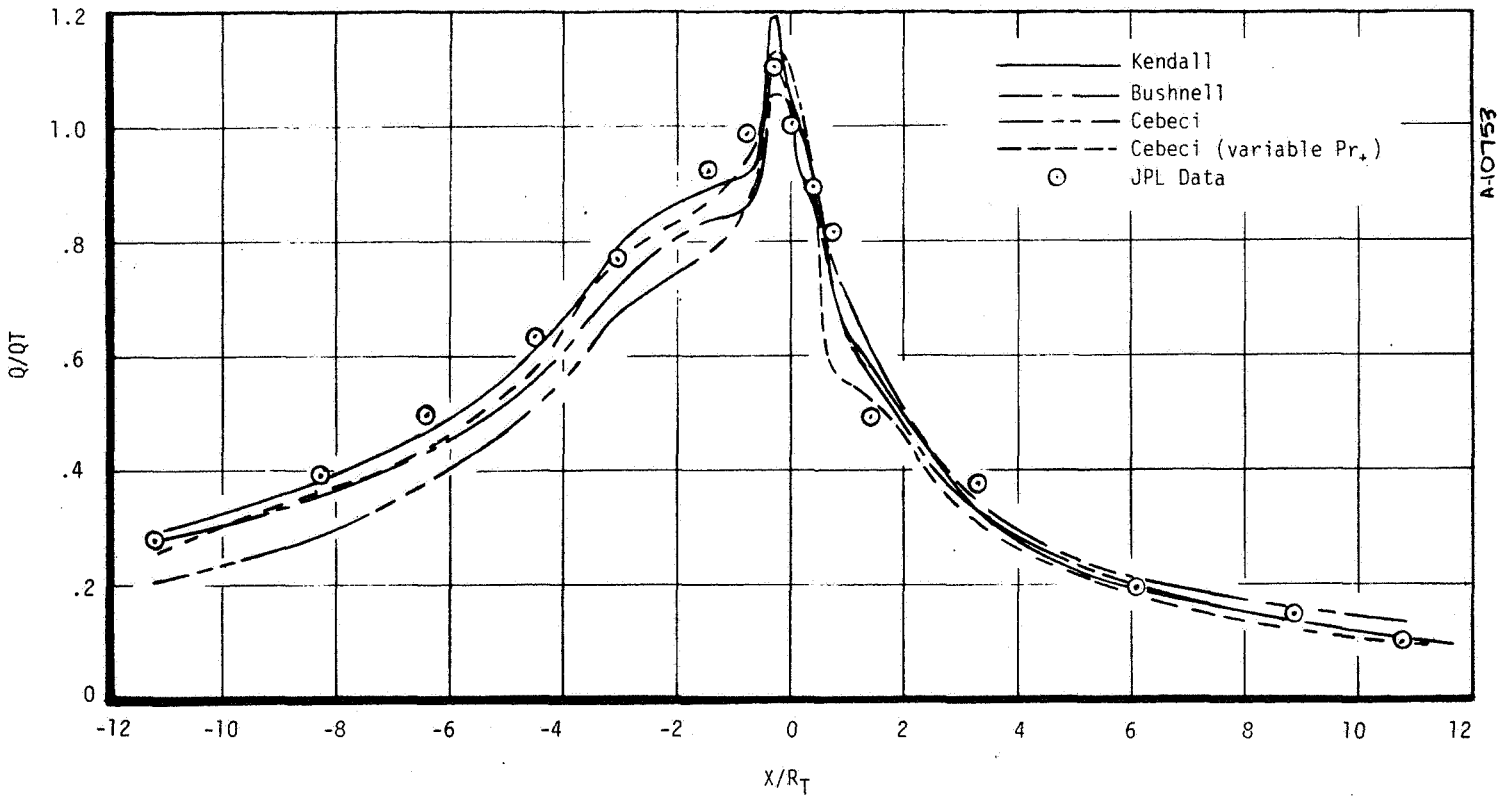

Figure 2. Comparison of wall heat flux for Back and Cuffel data.

Q_T = 5.4788 x 10^5 watts/m^2 (48.283 Btu/ft^2s)

R_T = 0.0202 m (0.06625 ft)

Re_θ = 6000 - 15,000

T_e/T_w = 0.7 - 2.0

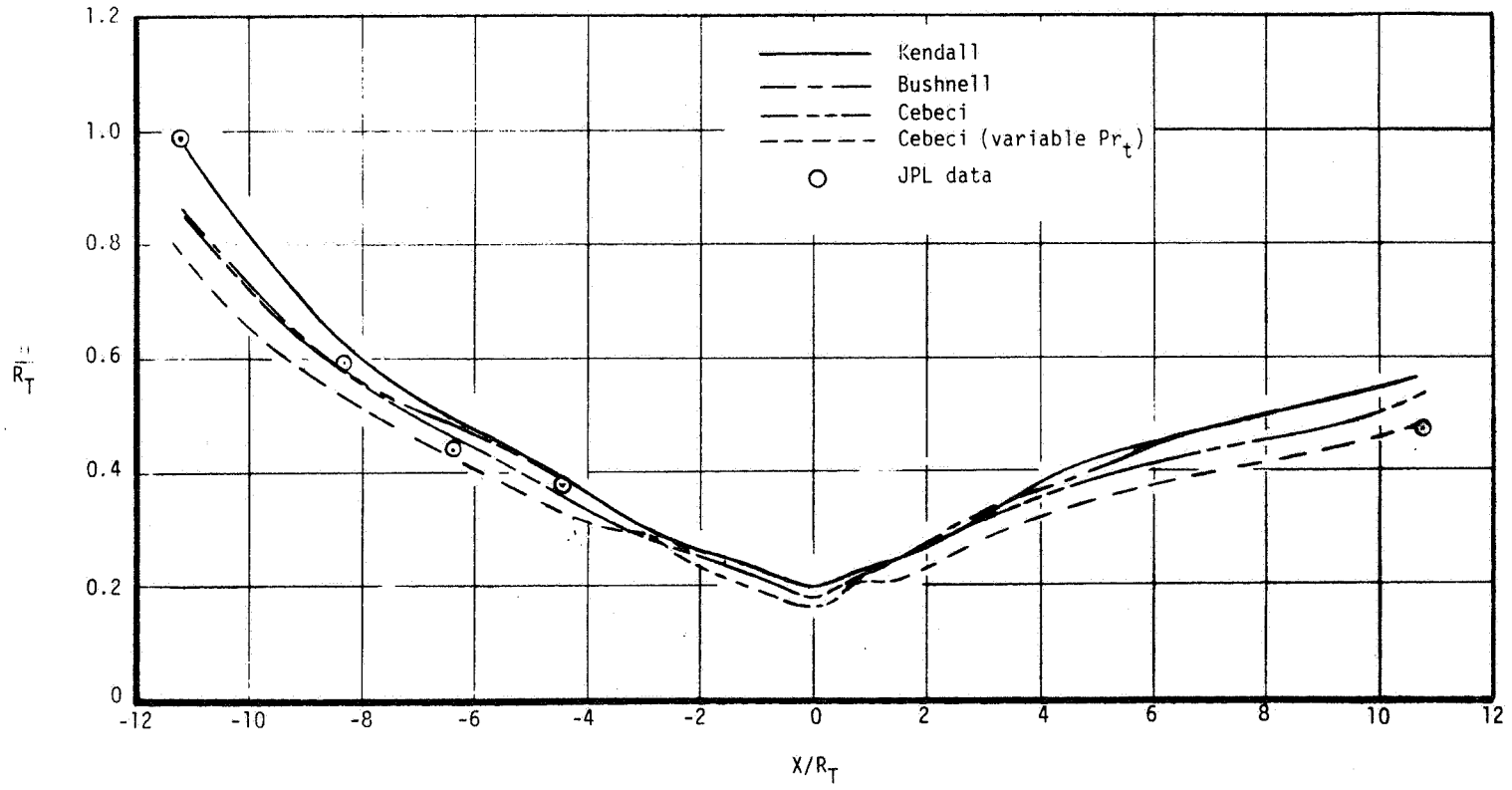

Figure 3. Comparison of momentum thickness for Back and Cuffel data.

R_T = 0.0202 m (0.06625 ft)

TABLE 1. BACK AND CUFFEL CASE, $x/R_T = -11.21$,
$\frac{Re}{\theta} = 2.1798 \times 10^7/m$ ($6.644 \times 10^6/ft$)

	Kendall	Bushnell	Cebeci	Cebeci (Variable PR_t)	Data
τ_w, N/m^2 (lbf/ft^2)	15.82 (0.3305)	14.18 (0.2961)	12.61 (0.2634)	13.64 (0.2849)	
$\dot{q}_w$, $watts/m^2$ (Btu/ft^2-s)	1.618×10^5 (14.26)	1.476×10^5 (13.01)	1.272×10^5 (11.21)	1.124×10^5 (9.906)	1.552×10^5 (13.68)
θ, m (ft)	1.84×10^{-3} (6.076×10^{-3})	1.743×10^{-3} (5.719×10^{-3})	1.607×10^{-3} (5.271×10^{-3})	1.593×10^{-3} (5.227×10^{-3})	2.006×10^{-3} (6.583×10^{-3})
δ^*, m (ft)	4.444×10^{-4} (1.458×10^{-3})	3.417×10^{-4} (1.121×10^{-3})	3.688×10^{-4} (1.21×10^{-3})	4.91×10^{-4} (1.611×10^{-3})	6.658×10^{-4} (2.25×10^{-3})

TABLE 2. BACK AND CUFFEL CASE, $x/R_T = 10.797$,
$\frac{Re}{\theta} = 4.111 \times 10^7/m$ ($1.253 \times 10^7/ft$)

	Kendall	Bushnell	Cebeci	Cebeci (Variable PR_t)	Data
τ_w, N/m^2 (lbf/ft^2)	214.98 (4.49)	207.2 (4.328)	185.0 (3.865)	209.6 (4.378)	
$\dot{q}_w$, $watts/m^2$ (Btu/ft^2-s)	6.445×10^4 (5.679)	6.387×10^4 5.628)	5.600×10^4 4.935)	7.014×10^4 (6.18)	5.752×10^4 (5.068)
θ, m (ft)	1.144×10^{-3} (3.754×10^{-3})	6.387×10^{-3} (3.77×10^{-3})	1.019×10^{-3} (3.344×10^{-3})	9.775×10^{-4} (3.207×10^{-3})	9.653×10^{-4} (3.167×10^{-3})
δ^*, m (ft)	9.933×10^{-4} (3.259×10^{-4})	2.31×10^{-5} (-7.58×10^{-5})	3.19×10^{-5} (1.089×10^{-4})	1.524×10^{-4} (5.0×10^{-4})	-3.048×10^{-4} (-1.0×10^{-3})

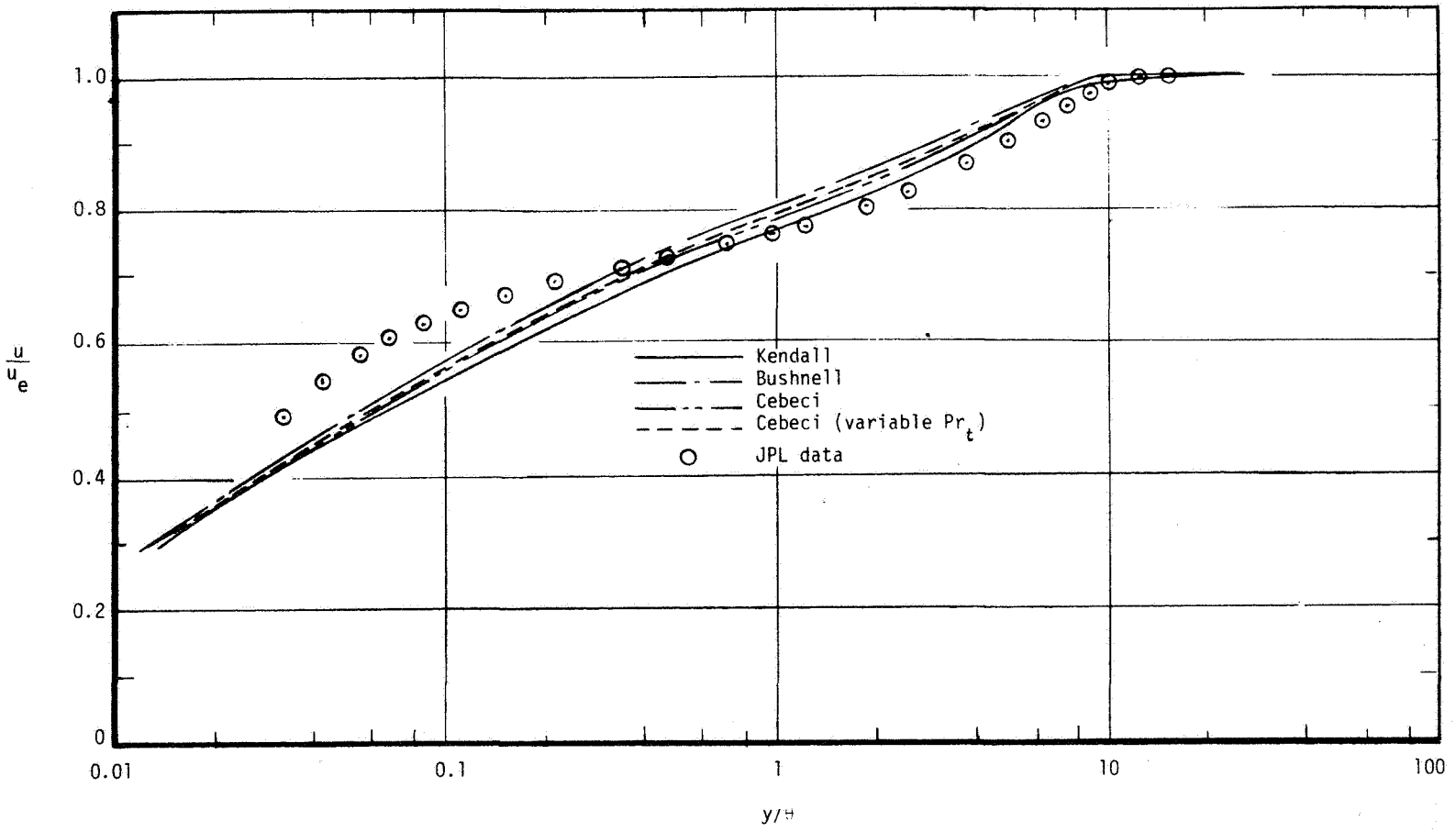

Figure 4. Comparison of velocity profiles for Back and Cuffel at x/R_T = -11.21

u_e = 42 m/s (138 ft/sec)

θ = 2.007 x 10^{-3} m (6.538 x 10^{-3} ft)

Re_θ = 8500

M = 0.07

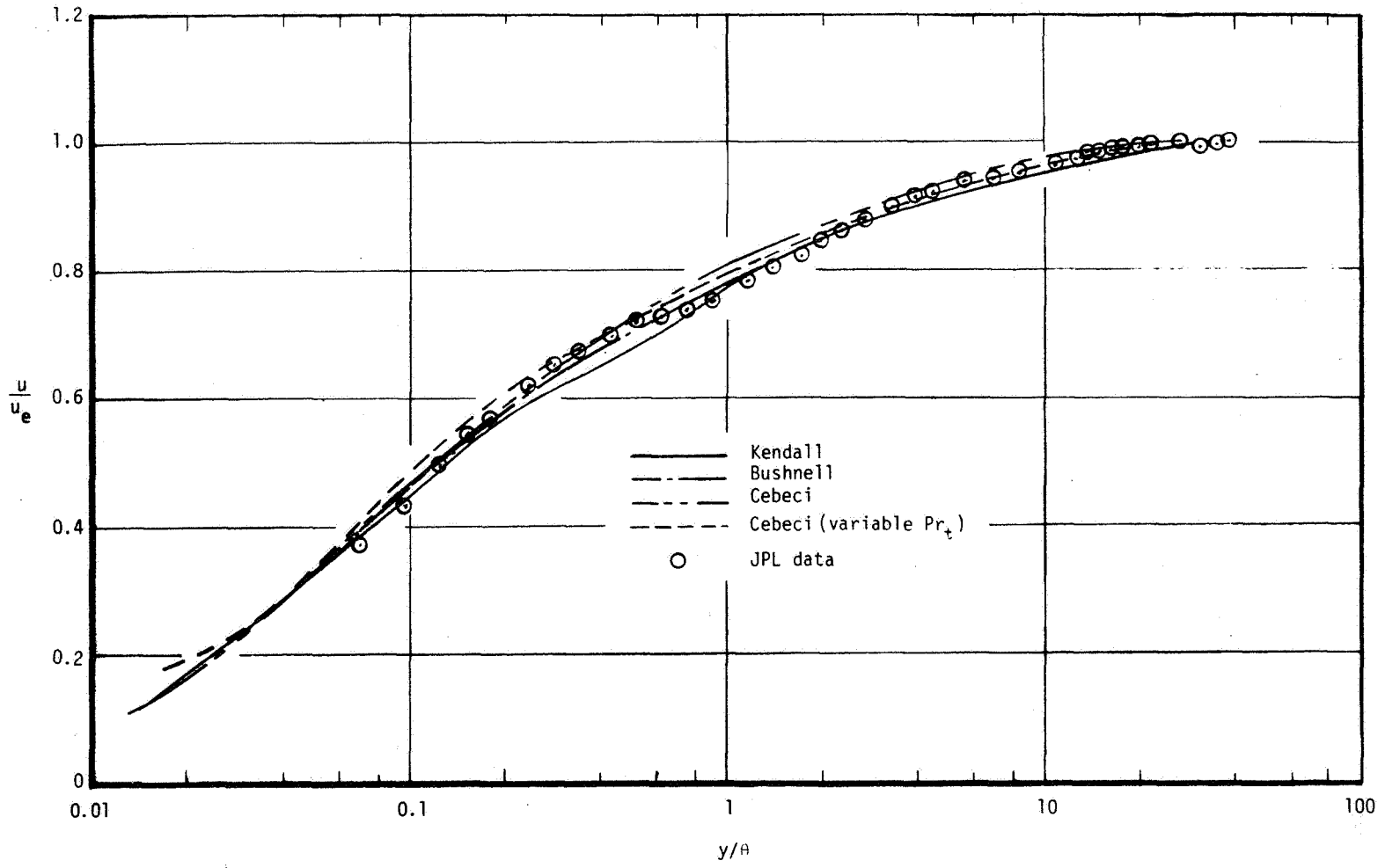

Figure 5. Comparison of velocity profiles for Back and Cuffel data at x/R_T = 10.797

u_e = 1100.9 m/s (3612 ft/s)

θ = 9.652 x 10^{-3} m (3.167 x 10^{-3} ft)

Re_θ = 15,000

M = 3.5

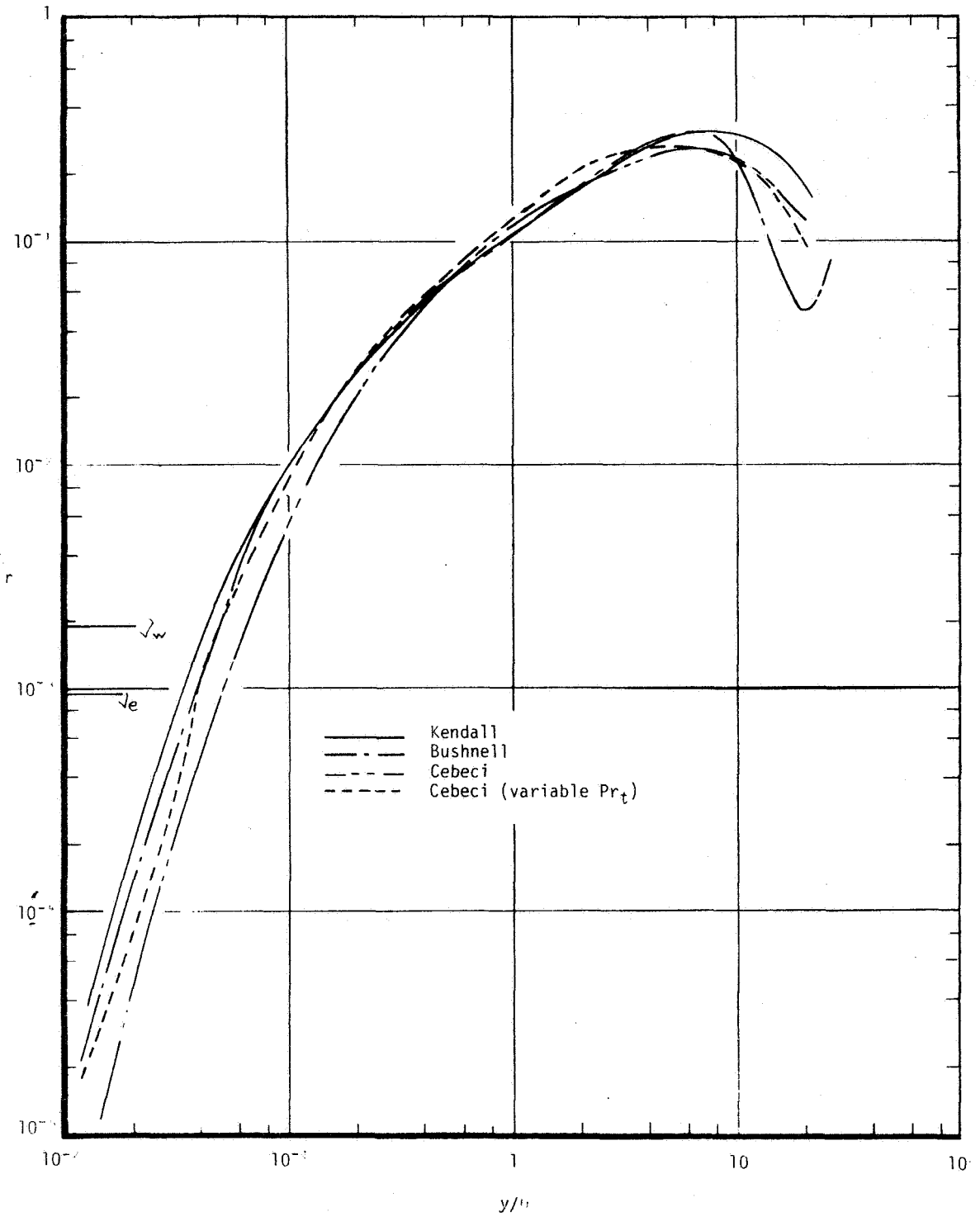

Figure 6. Comparison of eddy viscosity for Back and Cuffel case, $x/R_T = 10.797$.

$\theta = 9.655 \times 10^{-4}$ m (3.167×10^{-4} ft)

$\varepsilon_r = 0.0929$ m^2/s (1.0 ft^2/sec)

felt that comparative predictions would be of interest. Also, density variations (caused by temperature and species composition changes) of about a factor of 4 occur across the boundary layer and this was expected to be a possible cause for difference between the models. Values of Re_θ were between 1300 and 3600, much lower than the 4000 - 20,000 expected in SSME. It should be noted that this data is subject to uncertainty in the mixture ratio which make accurate comparison with predictions very questionable.

The nozzle geometry, fuel mixture ratio, stagnation conditions, calculated axial pressure variation, and wall temperature variation were provided. (The nozzle is 0.0762 m (0.25 ft) wide.) The stagnation conditions are given as:

$P_o = 4.6182 \times 10^6$ N/m^2 (45.57 atm)

$T_o = 3570°K$ (6430°R)

MR = 6.15

The injector plane was at the entrance to the nozzle and the initially low heat transfer shown by the data (Figure 7) was assumed to result from the presence of a liquid layer near the injector. Accordingly, the prediction was started downstream of the injector and assumed to have an established boundary layer at the starting position. The mixture ratio in the boundary layer was assumed to be 6.15. The heat flux data and the results of the BLIMP predictions are shown in Figure 7. The Kendall model is about 15 percent higher than the Bushnell model and the Cebeci model is about 6 percent lower. At the exit Kendall is about 38 percent higher and Cebeci is about 4 percent lower than the Bushnell. The predictions are for a fully turbulent boundary layer with a starting length of 0.0561 m (0.18406 ft). It should be noted that the flow was suspected of being of the laminarizing type. Also, the predicted values are sensitive to the mixture ratio. If the wall zone is fuel rich (lower mixture ratio) the predictions are uniformly lowered. The starting length is also an influential parameter. For these reasons no attempt was made to achieve better agreement with the data. Instead, the case was used to compare the three turbulent models for this type of flow, e.g., large edge temperature to wall temperature ratio (5 to 6) and chemical reactions. It is quite clear that the three models do not agree for this case. The velocity profiles are shown in Figure 8. The Kendall model is the most different of the three. This is attributed to the fact that the wall laws for the Bushnell and Cebeci models are very similar (of the Van Driest type) whereas the Kendall model is basically different, consisting of an integral-differential formulation. As discussed previously, Section 3.1.1, it was expected that these

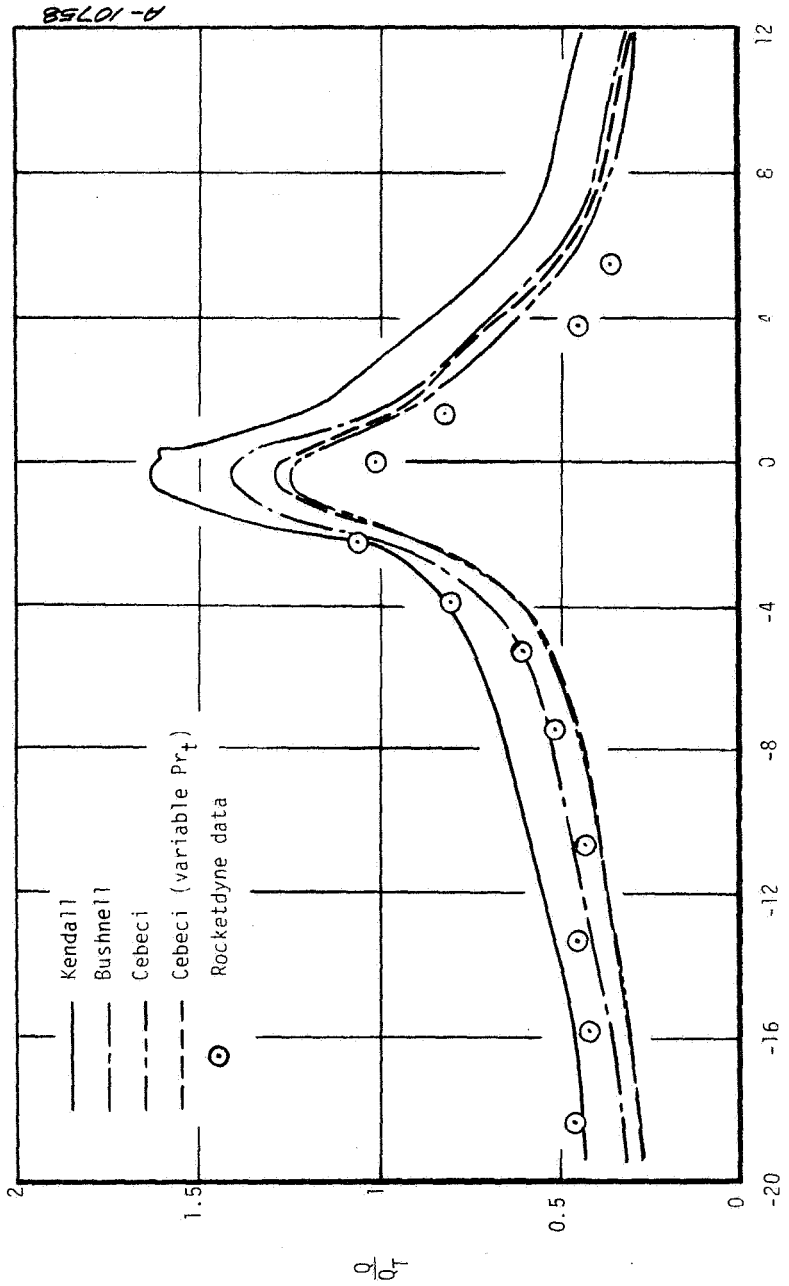

Figure 7. Comparison of wall heat flux for O_2/H_2 case.

Q_T = 4.053 x 10^7 watts/m^2 (3.571 x 10^3 Btu/ft^2s)
R_T = 3.93 x 10^{-3} m (1.289 x 10^{-2} ft)
Re_{ℓ} = 1300 - 3200
T_e/T_w = 4.5 - 6.0

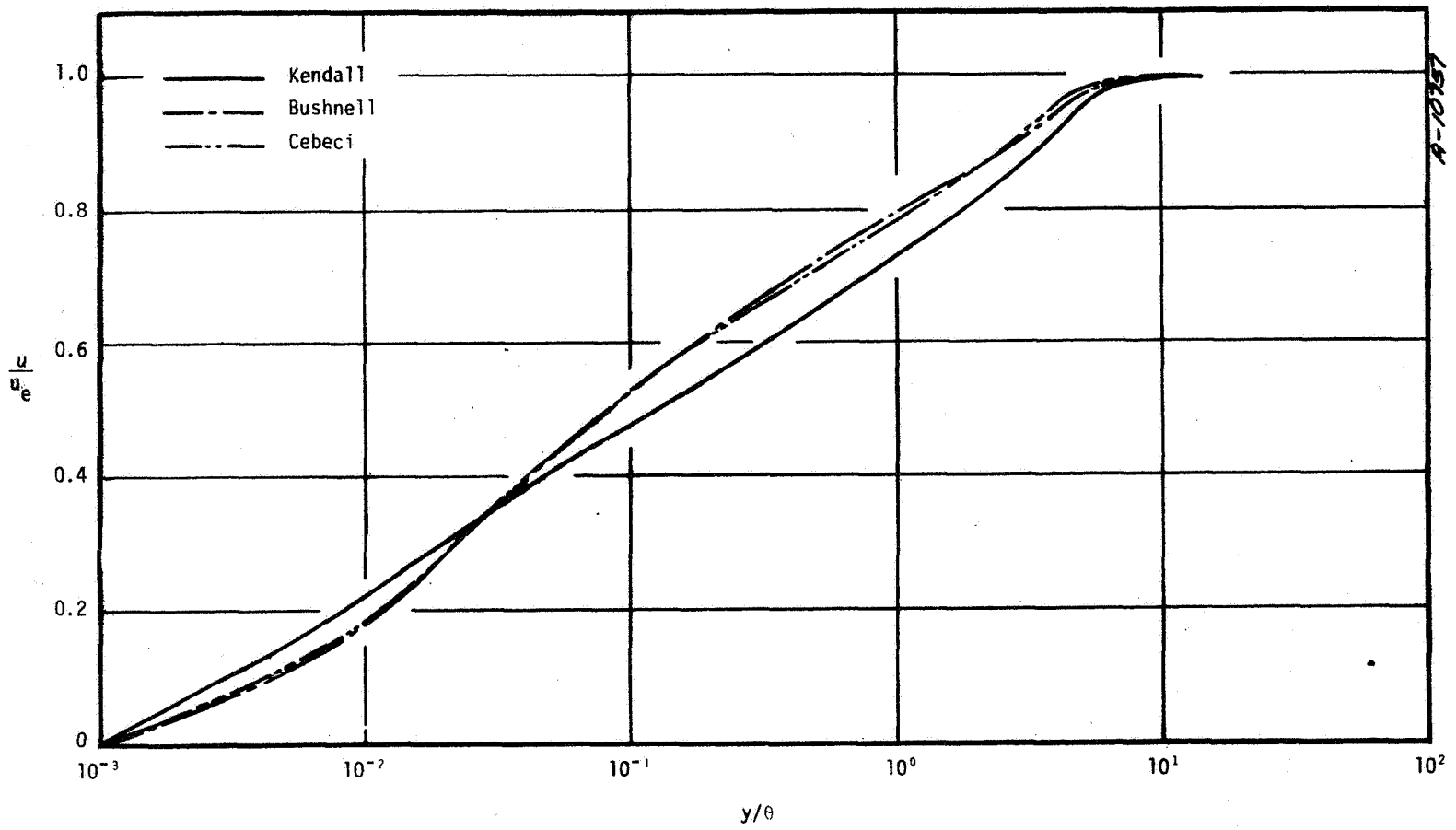

Figure 8. Comparison of velocity profiles for O_2/H_2 case, x/R_T = - 11.89

u_e = 3374 m/s (1.107×10^4 ft/s)

θ = 5.014×10^{-4} m (1.645×10^{-3} ft)

differences might become significant for large property variations through the boundary layer. The differences in the models are also apparent in Figure 9, which shows the eddy viscosity profiles. (The degree of property variation across the boundary layer is also indicated by the edge and wall values of kinematic viscosity.)

3.2.3 Hypothetical Cases

As a consequence of the differences observed in Section 3.2.2, the models were compared for several cases which would help to define the differences in the models. These cases and the results will be briefly summarized.

The comparison in Section 3.2.2 was for relatively low values or Re_θ and a severe pressure gradient. Therefore, the SSME flow conditions were used to compare the models at high Reynolds number ($2000 < Re_\theta < 20{,}000$) and less severe pressure gradient. Large values of T_e/T_w were used. The results were in agreement with those of Section 3.2.2. The Kendall model was between 25 and 40 percent higher in wall heat flux than the other two models.

The effects of property variation only were examined by using a zero pressure gradient, $Re_\theta = 6000$ air flow case for $T_e/T_w = 5$ and $T_e/T_w = 0.2$. For the large values of T_e/T_w the results were again similar to the Rocketdyne and SSME cases. However, for $T_e/T_w \approx 0.2$ the models were in very close agreement. Examination of the profiles (for $T_e/T_w \approx 0.2$) revealed that most of the property variation occurred in the wake portion of the boundary layer. (Viscous heating maintained the temperature near the wall value in the inner region of the boundary layer.) Since the Kendall and Cebeci models are identical in the wake no differences should occur if the wall region is approximately a constant property region. This further confirmed that it is for large property variations in the law of the wall region that the models disagree.

As a further test for large property variations with large Re_θ, the Back and Cuffel case was rerun with the wall temperature reduced so that $T_e/T_w \approx 5$. The results were the same as in all the previous cases of large T_e/T_w.

3.2.4 Flow Over a Hemisphere-Cylinder

At the time the turbulent models were being examined some experimental data from AEDC* were made available. This data was for M = 12 air flow over a hemisphere (0.0635 m radius) with a cylindrical afterbody. Over the region of interest Re_θ was less than 300. The body

*Unpublished data, provided courtesy Mr. Emmitt Edenfield, Arnold Engineering and Development Center.

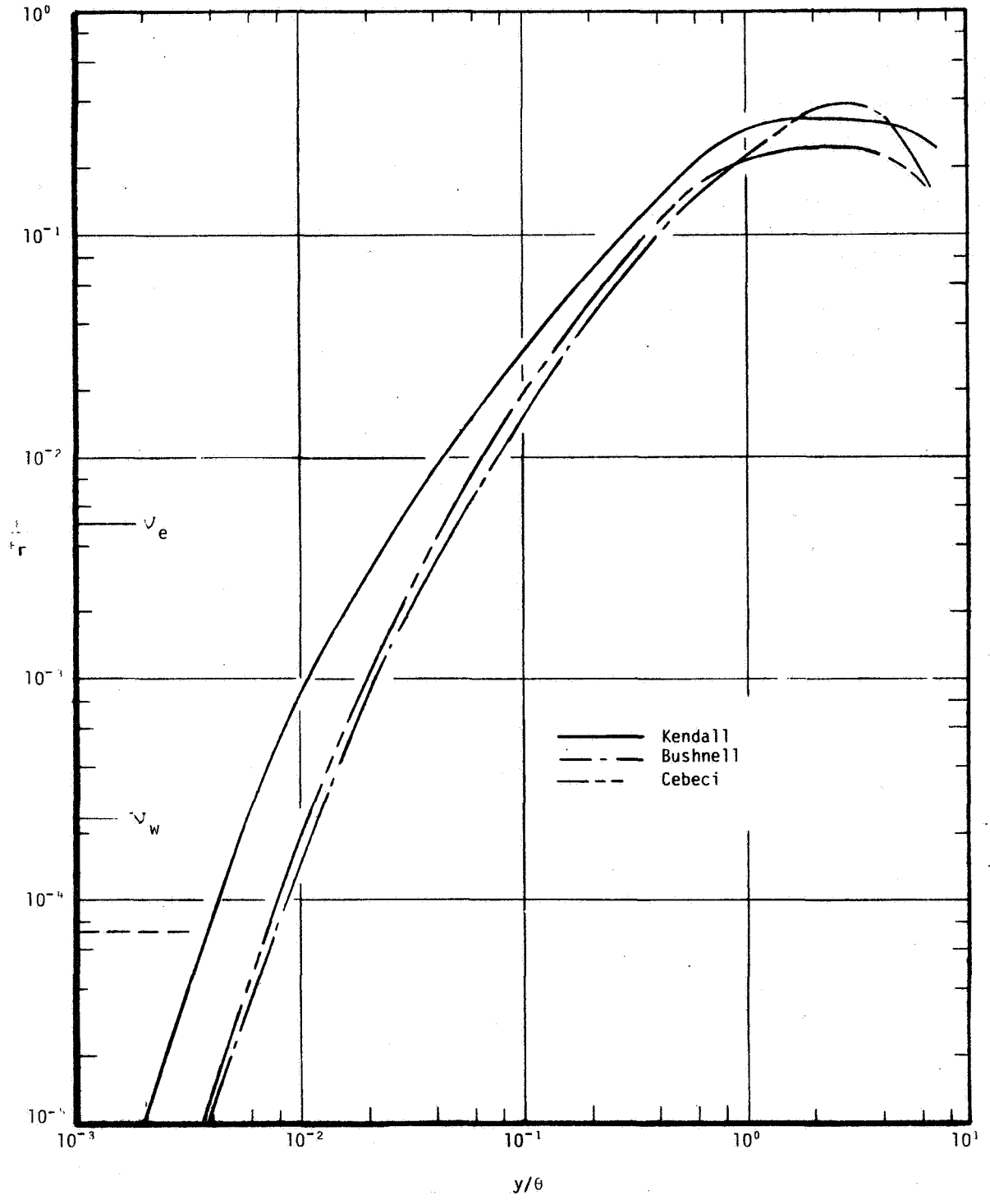

Figure 9. Comparison of eddy viscosities for O_2/H_2 case, x/R_T = -11.89.

θ = 5.014 x 10^{-4} m (1.645 x 10^{-3} ft)

ε_r = 0.0929 m^2/s (1.0 ft^2s)

shape and pressure distribution are shown in Figure 10. The interesting feature of this data was that the ratio T_e/T_w varied from 5.2 to 2.0. BLIMP predictions for this data using an external flow option in another version of BLIMP were made. The flow over the hemisphere was artificially tripped at $S/R_o \approx 0.2$ on one side of the hemisphere. (The BLIMP predictions for heat flux for the laminar flow along the untripped side were in excellent agreement with the data.) The heat flux predictions for the turbulent flow for the Kendall and Bushnell models are shown in Figure 11. The Cebeci model is approximately the same as the Bushnell model. In the region of large T_e/T_w the Kendall model is as much as 40 percent larger than the Bushnell model.

This single comparison is not considered as conclusive because the data is not of the type desired for verification of a turbulent model. First, the models are not considered to be well tuned for low Reynolds number flows and second, there is some evidence that in the region immediately downstream of transition there is an increase in turbulent mixing that has not been taken into account in the models. Although part of the differences in the predictions of the models can be attributed to the severe property variations, the agreement with the data by the Kendall model may be fortuitous.

3.3 COMPARISON OF COMPUTATION TIME

There are many factors that effect the execution time of each model — the starting profile, the degree of nonsimilarity, etc. Each model performs differently in any given situation. For the several problems considered there was no clear indication of which model is fastest. The time per iteration is usually slightly more for the Bushnell model (~10 percent) than for the Cebeci or Kendall models, which are about the same. However, the number of iterations does not consistently favor any of the models. For example, in the three cases initially considered (JPL data, Rocketdyne O_2/H_2 case, and SSME model air flow) a different model had the shortest overall execution time for each case. Thus, there does not appear to be a strong motive to select any model based on computation time.

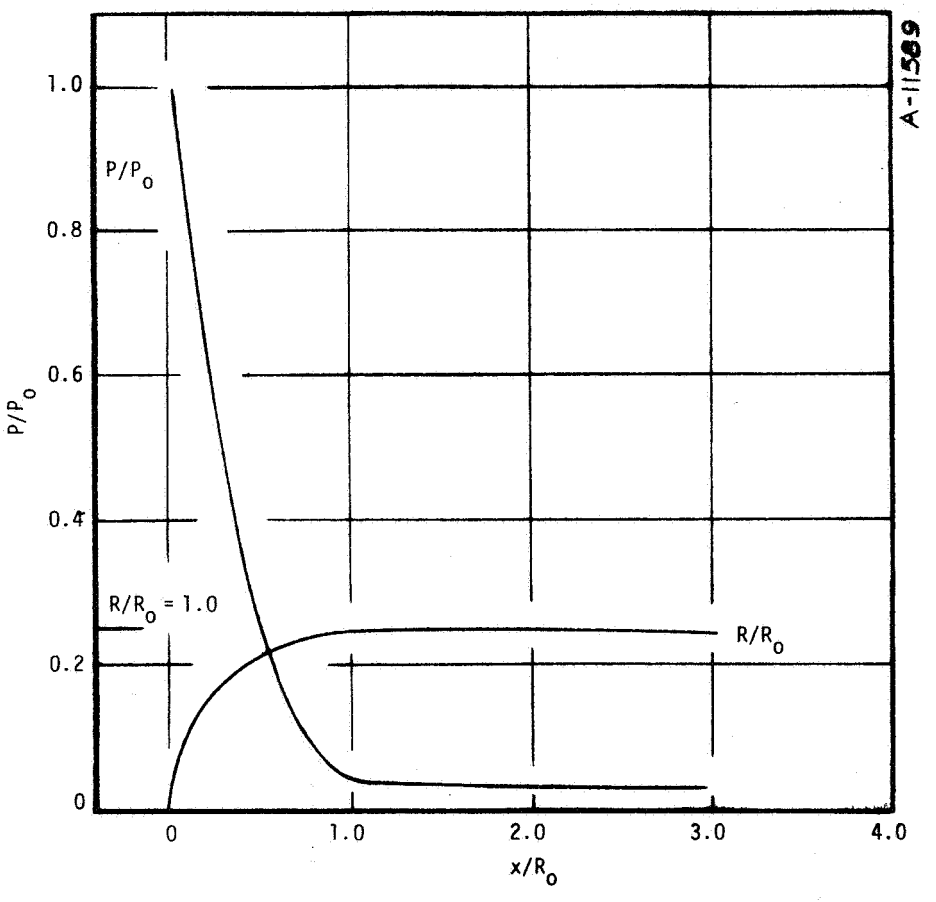

Figure 10. Body shape and pressure distribution for AEDC hemisphere cylinder.

$M = 12$

$R_0 = 0.0635$ m (2.5 in.)

$P_0 = 1.94 \times 10^5$ N/M^2 (1.912 atm)

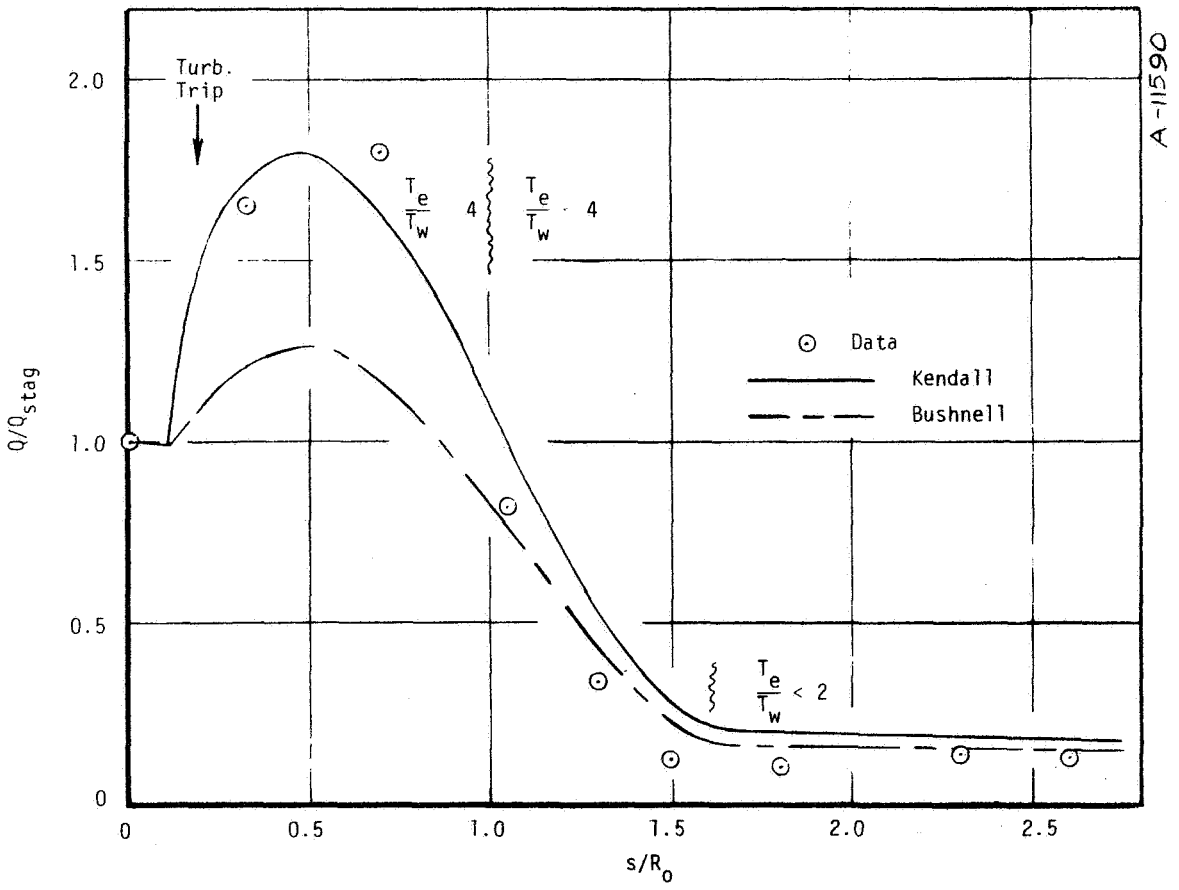

Figure 11. Heat flux for AEDC hemisphere cylinder.

M = 12

R_o = 0.0635 m (2.5 in.)

Q_{stag} = 8.74 x 10^5 watts/m^2 (77 Btu/ft^2s)

SECTION 4

CONCLUSIONS

The major conclusions of this work pertain to the turbulent model study and are given below.

- For nonreacting flows with moderate pressure gradients (i.e., not severe enough to cause laminarization) and values of $T_e/T_w \lesssim 3$ the three models are equivalent and seem to agree with the data.
- For nonreacting flows with large values of T_e/T_w (≈ 5), the Kendall model does not agree with the Cebeci or Bushnell models. The Kendall model predicts significantly higher values of heat flux.
- The Kendall model should remain as the standard model for prediction of boundary layer effects in liquid rocket engine thrust chambers since it is the model that was initially incorporated in the BLIMP program. It is imperative that data be obtained to resolve the question of large property variations in the "law of the wall" region.

SECTION 5

RECOMMENDATIONS

1. The importance of gas phase kinetics on the prediction of wall heat flux thrust loss, and body displacement should be assessed. If kinetics prove to have significant effects, a means to include kinetics in BLIMP-J should be investigated.

2. The capability to freeze the chemical composition at any point in the expansion should be added to BLIMP-J. Currently BLIMP-J can be run either with a completely equilibrium chemistry or with frozen chemistry. This option would allow the user to mix the two options. For example, equilibrium chemistry might be used upstream of the throat, and the composition frozen at the throat values for the expansion.

3. A parametric study to determine the sensitivity of the predictions to certain input values should be made. Two of the most obvious parameters are the mixture ratio and the initial starting length for the boundary layer.

4. The importance of laminarization for the rocket nozzles of interest should be assessed. The current turbulent models do not appear to adequately model this effect; although a rigorous comparison with data has not been made. If laminarization is important, adequate means to model it should be investigated. This could include modification to the current models in BLIMP or the addition of a suitable turbulent kinetic energy model.

5. In view of the differences in predictions of the three turbulent models for the case of large T_e/T_w, suitable data should be identified and comparisons made. If no such data are available then an experimental program should be designed and conducted.

REFERENCES

1. "JANNAF Rocket Engine Performance and Evaluation Manual," CPIA Publication 246, April 1975.

2. Evans, R. M., "Boundary Layer Integral Matrix Procedure for JANNAF Rocket Engine Performance Evaluation Methodology, User's Manual — BLIMP-J" Aerotherm UM-75-64, Aerotherm Division/Acurex Corporation, Mt. View, California, July 1975.

3. Kendall, R. M., Anderson, L. W., and Aungier, R. H. "Nonsimilar Solution for Laminar and Turbulent Boundary-Layer Flows over Ablating Surfaces," AIAA Vol. 10, No. 9, September 1972, page 123-1236.

4. Anderson, L. W. and Morse, H. L., "A Turbulent Model Study for the Multicomponent Nonsimilar Turbulent Boundary Layer Program," Air Force Weapons Laboratory Technical Report No. AFWL-TR-57, October 1971.

5. Cebeci, T. and Smith, A.M.O., "A Finite-Difference Method for Calculating Compressible Laminar and Turbulent Boundary Layers," Journal of Basic Engineering, Paper No. 70-FE-A, 1970.

6. Cebeci, T., "A Model for Eddy-Conductivity and Turbulent Prandtl Number," Report No. MDC-J0747/01, McDonnell-Douglas, Corp., May 1970.

7. Beckwith, I. E., and Bushnell, D. M., "Calculation by a Finite-Difference Method of Supersonic Turbulent Boundary Layers with Tangential Slot Injection," NASA TN-D-6221, April 1971.

8. Harris, J. E., "Numerical Solution of the Equations for Compressible Laminar, Transitional, and Turbulent Boundary Layers and Comparisons with Experimental Data," NASA TR-R-368, April 1971.

9. Evans, R. M. and Morse, H. L., "Boundary Layer Integral Matrix Procedure Code Modifications and Verifications," Aerotherm Division/Acurex Corporation, Final Report 74-95, Mt. View, California, March 1974.

10. Nickerson, G. R., Coats, D. E., and Bartz, J. L., "Two Dimensional Kinetic Reference Computer Program," Ultra Systems, Inc., Irvine, California, December 1973 (NASA Contract NAS 9-12652).

11. Kendall, R. M., Rubesin, M. W., Dahm, T. J., and Mendenhall, M. R., "Mass Momentum, and Heat Transfer Within a Turbulent Boundary Layer with Foreign Gas Mass Transfer at the Surface, Part I — Constant Fluid Properties," Final Report No. 111, Vidya/Itek Corporation, February 1964.

12. Van Driest, E. G., "On Turbulent Flow Near a Wall," Journal of Aero. Sci., Vol. 23, 1956, p. 1007.

13. Simpson, R. L., Kays, W. M., and Moffat, R. J., "The Turbulent Boundary Layer on a Porous Plate: An Experimental Study of Fluid Dynamics with Injection and Suction," Report No. HMT-2, Stanford University, Stanford, California, December 1967.

14. Johnson, D. S., "Velocity and Temperature Fluctuations in a Turbulent Boundary Layer Downstream of a Stepwise Discontinuity in Wall Temperature," J. Appl. Mech., Vol. 26, 1959, p. 325.

15. Ludweig, H., "Bestimmung des Verhaltnisses der Austauschkoeffizienten fur Warme und Impuls bei Turbulenten Grenzschiechten," Z. Flugwiss, Vol. 5, 1956, p. 73.

16. Klebanoff, P. S., "Characteristics of Turbulence in a Boundary Layer with Zero Pressure Gradient," NACA Report 1247, 1955.

17. Bushnell, D. M. and Beckwith, I. E., "Calculation of Nonequilibrium Hypersonic Turbulent Boundary Layers and Comparisons with Experimental Data," AIAA, Vol. 8, No. 8, 1970, p. 1462.

18. Peterson, J. B., Jr., et al., "Further Investigation of Effect of Air Injection Through Slots and Porous Surfaces on Flat Plate Turbulent Skin Friction at Mach 3," NASA TN D-331, March 1966.

19. Jeromin, L. O. F., "An Experimental Investigation of the Compressible Turbulent Boundary Layer with Air Injection," A.R.C., Volume 28, London, England, November 1966, p. 549.

20. Back, L. H. and Cuffel, R. F., "Turbulent Boundary Layer and Heat Transfer Measurements Along a Convergent-Divergent Nozzle," Journal of Heat Transfer, November 1971, pp. 397-407.